Supplement of:
Numerical modelling of permafrost spring discharge and open-system pingo formation induced by basal permafrost aggradation

Mikkel T. Hornum[1,2], Andrew J. Hodson[1,3], Søren Jessen[2], Victor Bense[4], Kim Senger[1]

[1]Department of Arctic Geology, The University Centre in Svalbard (UNIS), N-9171 Longyearbyen, Norway.
[2]Department of Geosciences and Natural Resource Management, University of Copenhagen, 1350 Copenhagen K, Denmark.
[3]Department of Environmental Science, Western Norway University of Applied Sciences, N-6856 Sogndal, Norway
[4]Department of Environmental Sciences, Wageningen University, 6708PB Wageningen, Netherlands.

Correspondence to: Mikkel T. Hornum (mth@ign.ku.dk)

S1 Modelling approach

Figure S1 provides a schematic overview of the inner workings of the decoupled heat and groundwater model applied in the investigation. The 1D heat transfer model (1DHT) is connected to the 3D steady-state groundwater model by a source term defined by the rate of permafrost aggradation (Eq. 6).

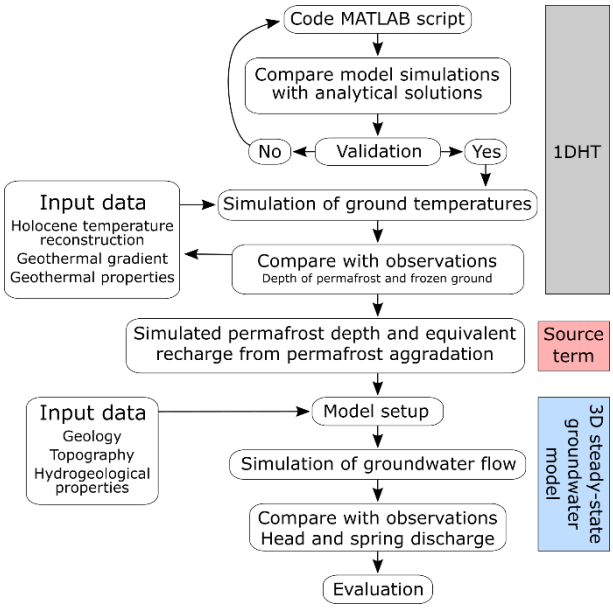

Figure S1 Schematic overview of the inner workings of the decoupled heat and groundwater model.

S2 Validation of the 1DHT model

The 1D heat transfer model (1DHT) consists of a MATLAB script (MathWorks®, 2019) tailored to simulate dynamics of ground temperatures and permafrost conditions. The model code is publically available at DOI:10.5281/zenodo.3578839.

Before the 1HDT model was applied in our investigation, it was validated through comparison with two analytical solutions. In the following, we first describe the basis of the 1DHT model. Second, we present two different analytical solutions and show how they compare with numerical results as simulated by the 1DHT model.

S2.1 Model code

In the core of the 1DHT model is an explicit forward-difference time approximation of the one-dimensional conductive heat transfer (Eq. 1). For the interior cell, i, which is situated in a 1D grid in all of which the initial temperature, T^p, is known (Fig. S1), this approximation states that at a new time, $(p+1)$,

$$\frac{T_i^{p+1}-T_i^p}{\Delta t} = \alpha \frac{T_{i+1}^p - T_i^p + T_{i-1}^p}{\Delta x^2}$$

$$\Leftrightarrow \quad T_i^{p+1} = \frac{\alpha\,\Delta t}{\Delta x^2}\left(T_{i+1}^p + T_{i-1}^p\right) + \left(1 - 2\frac{\alpha\,\Delta t}{\Delta x^2}\right) T_i^p \qquad \text{(S1)}$$

where T_i^{p+1} is the temperature in cell i at the time $(p+1)$, Δt is the time step, and Δx is the distance to the center of the neighboring cells. The thermal diffusivity, α, is calculated as defined by Eqs. (1), (3), and (4) in Sect. 4.1. Equation S1 is only a stable numerical solution if the stability criterion is true (Bergman et al., 2011):

$$\frac{\alpha\,\Delta t}{\Delta x^2} \le \frac{1}{2} \quad \Leftrightarrow \quad \Delta t \le \frac{\Delta x^2}{\alpha}\frac{1}{2} \qquad \text{(S2)}$$

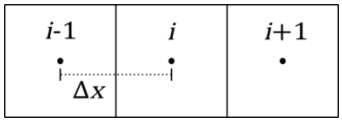

Figure S2 Conceptual representation of a 1D grid for which the 1DHT model simulates temperature changes (Eq. S1).

S2.2 Neumann's solution

In the case of phase change, conductive heat transfer becomes non-linear and the mathematical (Stefan) problems that arise may be of considerable difficulty (Carslaw and Jaeger, 1959). One of the exact solutions that deal with such a problem is the Neumann solution, which here is presented largely based on Mottaghy and Rath (2006). The presented version of the Neumann solution solves the 1D heat equation (Eq. 1), for a semi-infinite body, which consists of a single component and initially has the liquidus temperature. At the surface, the body is exposed to a negative temperature step change and the medium starts to change phase from liquid to solid. The position of the phase front, Z, is expressed as a function of time, t:

$$Z(t) = 2 \cdot \gamma \cdot \sqrt{\alpha_{so} \cdot t} \qquad \text{(S3)}$$

where γ is a parameter determined by

$$\frac{\left(\exp\left((\alpha_{so}-\alpha_{li})\cdot\frac{\gamma^2}{\alpha_{li}}\right)\cdot \mathrm{erfc}\left(\gamma\cdot\sqrt{\frac{\alpha_{so}}{\alpha_{li}}}\right)\right)}{\mathrm{erf}(\gamma)} - \frac{\left((T_L-T_S)\cdot k_{li}\cdot\sqrt{\alpha_{so}}\right)}{(T_S-T_0)\cdot k_{so}\cdot\sqrt{\alpha_{li}}} = 0 \quad \text{(S4)}$$

In both above equations, α's are thermal diffusivities, k's are thermal conductivities, and subscripts so and li refer to the solid or liquid state. T_L and T_S are the liquidus and solidus temperatures and T_0 is the surface temperature at $t > 0$. The latent heat of fusion is incorporated in the expression of the thermal diffusivity of the liquid:

$$\alpha_{li} = \frac{k_{li}}{\rho_{li}\cdot c_{li} + L\frac{-1}{T_L-T_S}} \quad \text{(S5)}$$

where ρ_{li} and c_{li} is the liquid's density and specific heat capacity, respectively.

To compare the 1DHT model with the exact Neumann's solution (Eq. S3), a situation which can be handled by both methods, was defined: A body of pure water, initially at the liquidus temperature $T_L = 0$ °C is exposed to a surface temperature of $T_0 = -4$ °C for a period of 3000 yr. The thermal properties of ice and water are as listed Table 1 and the solidus temperature is $T_S = -2$ °C. In the following, these conditions will be referred to as Neumann conditions.

Solving Eq. S4 with the Neumann conditions, we found that $\gamma = 0.0679$. Numerically, the 1DHT model simulated the temperature development in a 1D-grid containing 100 cells each with a length of 2 m. From the model simulation results, the propagation of the freezing front was evaluated by interpolating $T = -2$ °C. The propagation of the freezing front, as calculated by Neumann's solution and evaluated from the 1DHT model simulation, is plotted on Fig. S2. The RMSE of the simulation results is 0.011 and show a relatively good model performance.

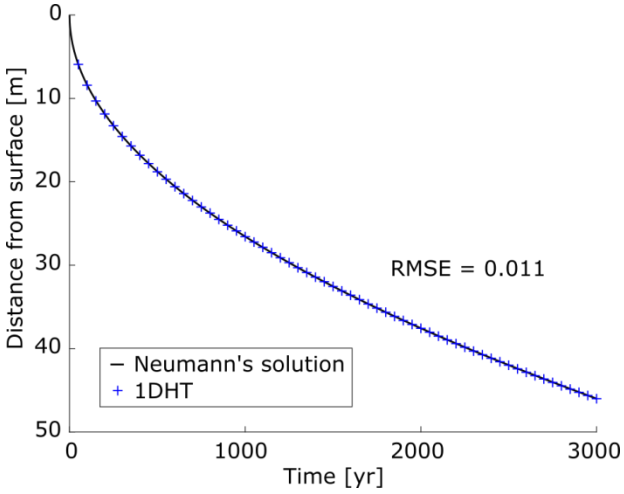

Figure S3 Freezing front depth with time in a body of water under Neumann conditions (see text) as calculated by the numerical 1DHT model and the analytical Neumann's solution.

S2.3 Step change in surface temperature (no latent heat effects)

This analytical solution also assumes a negative temperature step change at the surface of a semi-infinite body: At the time t=0, the surface temperature is T_{0i}, and at any later times ($t > 0$), it is T_0. As opposed to Neumann's solution, latent heat effects are neglected, but the initial medium (e.g. ground) temperature can follow any (uniform) geothermal gradient and the medium may consist of several components. Following the step change in surface temperature ($\Delta T_0 = T_0 - T_{0i}$), the temperature change, ΔT, is described as a function of time, t, and depth, z, by (Carslaw and Jaeger, 1959; Eppelbaum et al., 2014):

$$\Delta T(z,t) = \Delta T_0 \cdot \mathrm{erfc}\left(\frac{z}{2\cdot\sqrt{\alpha_{eff}\cdot t}}\right) \quad \text{(S6)}$$

where α_{eff} is the effective thermal diffusivity. As with Neumann's solution, it was necessary to describe conditions, which this analytical solution can handle. The initial surface temperature was defined as $T_{0i} = 5$ °C and the ground temperature distribution followed a geothermal gradient of 0.025 °C m^{-1}. At times $t > 0$, the surface temperature was defined as $T_0 = 0°C$ implying that $\Delta T_0 = -5$ °C. The medium had the geothermal properties of silty sand (Table 2) and a total porosity n=0.4, which was fully saturated with water. This yields $\alpha_{eff} = 5.7$ m^2 yr^{-1}.

The numerical grid was set up as for the simulation of the Neumann conditions except for the temperature distribution, which followed the geothermal gradient as described above. The calculated ground temperature distribution from both the 1DHT model and the analytical solution at $t = 1000$ yr is presented on Fig. S3. An excellent performance by the 1DHT model is indicated by a RMSE of $1.3 \cdot 10^{-5}$.

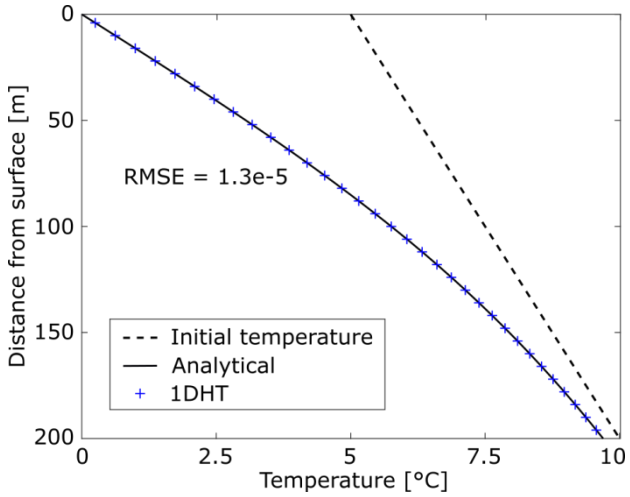

Figure S4 Comparison of the ground temperature distribution at $t = 1000$ yr calculated analytically (Eq. S6) and as simulated by the 1DHT model.

S3 Major ions in Adventdalen pingo spring waters

Hydrochemical data from 25 spring water samples from 2014 to 2017 presented by Hodson et al. (In Review) and publically available from DOI:10.5285/3d82fd3f-884b-47b6-b11c-6c96d66b950d give insights into the groundwater system in Adventdalen. As illustrated in Fig. S5a, water samples from Lagoon (LP), Førstehytte (FHP), Innerhytte (IHP) and River Pingos (RP) reveal that all these springs share the same sodium-bicarbonate ($NaHCO_3$) water type. The only exception is four samples taken near River Pingo in 2017 of a magnesium-sulfate water type (Fig. S5b). These four samples were excluded from the discussion because they might not be associated with a pingo according to Hodson et al. (In Review).

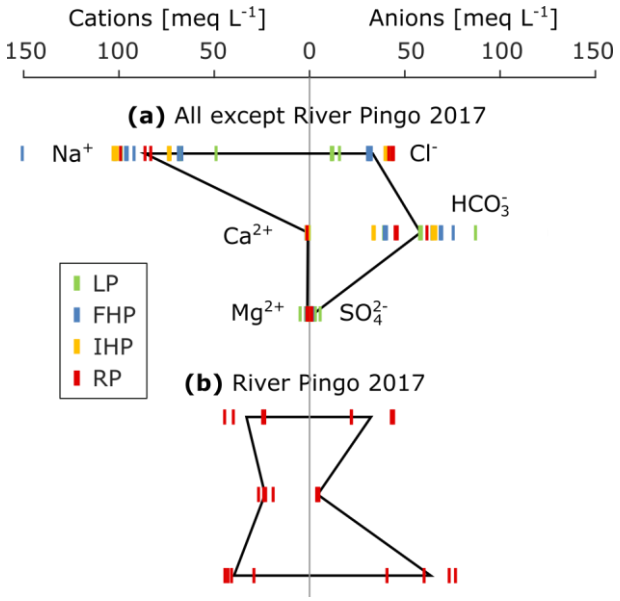

Figure S5 Stiff plots of major ion concentrations from pingo spring water samples in Adventdalen (data first presented in Hodson et al., In Review). The corners of the Stiff polygons represent mean concentrations.

References

Bergman, T. L., Lavine, A. S., Incropera, F. P. and Dewitt, D. P.: Fundamentals of Heat and Mass Transfer, 7th ed., John Wiley & Sons., 2011.

Carslaw, H. S. and Jaeger, J. C.: Conduction of heat in solids, 2nd ed., Clarendon Press., 1959.

Eppelbaum, L., Kutasov, I. and Pilchin, A.: Applied Geothermics, Lect. Notes Earth Syst. Sci., 757, doi:10.1007/978-3-642-34023-9, 2014.

Hodson, A., Nowak, A., Senger, K., Redeker, K. R., Christiansen, H. H., Jessen, S., Hornum, M. T., Betlem, P., Thornton, S.,

Turchyn, A. V., Olaussen, S. and Marca, A.: Open system pingos as hotspots for sub-permafrost methane emission in Svalbard, Cryosph. Discuss., doi:10.5194/tc-2020-11, in review, 2020.

MathWorks®: MATLAB R2019b, [online] Available from: https://se.mathworks.com/products/matlab.html, 2019.

Mottaghy, D. and Rath, V.: Latent heat effects in subsurface heat transport modelling and their impact on palaeotemperature reconstructions, Geophys. J. Int., 164(1), 236–245, doi:10.1111/j.1365-246X.2005.02843.x, 2006.